Heterostructures Based on Thin Films of Lanthanum Manganites and Multiferroic Bismuth Ferrite

Bonifacas VENGALIS [*], Kristina ŠLIUŽIENĖ

Center forPhysical Sciences and Technology, Semiconductor Physics Institute, Goštauto 11, LT-01108 Vilnius, Lithuania

We review results of our recent investigations on preparation and electrical properties of thin films and heterostuctures of colossal magnetoresistance manganites and multiferroic $BiFeO_3$ (BFO). Major attention is paid to the interfaces formed between the oxides, conducting $SrTiO_3<Nb>$ and semiconducting organic (Alq3) compound. Thin films of $La_{2/3}A_{1/3}MnO_3$ (A = Ca, Sr, Ba, Ce) and BFO were grown by magnetron sputtering on conducting lattice-matched Nb-doped $SrTiO_3$ substrates while the organic films were prepared as top layers onto the oxide layers by thermal evaporation. Nonlinear electrical properties and magnetoresistance of the heterostructures have been investigated in a wide temperature range (78 K – 400 K). Various mechanisms, i. e. thermoionic emission in a barrier of Schottky type, carrier tunneling through the interfaces and space charge limited current processes were considered to explain nonlinear electrical transport properties in the heterojunctions. Both negative and positive magnetorestance values have been indicated for the heterojunctions formed by growing the manganite films on $SrTiO_3<Nb>$ substrates. The Alq3/LSMO heterojunctions demonstrated magnetoresistance values up to 11 % (at $T = 240$ K and $B = 1$ T).

Keywords: thin film growth, manganites, heterostructures, organic semiconductor, Alq3, interface engineering, electrical resistance, magnetoresistance

1. INTRODUCTION

During the last decade, considerable progress has been made in fabrication, research and application of new device structures based on thin films of functional oxides with correlated electronic systems. This group of oxides includes high T_c superconducting cuprates, colossal magnetoresistance manganites, a number of ferromagnetic, ferroelectric, multiferroic oxides and great variety of other complex oxide systems [1].

Perovskite manganites referred to by the general formula $Ln_{1-x}A_xMnO_3$, (here Ln = La, Nd,…, and A is a divalent cation such as Ba, Sr or Ca) have received considerable attention in recent years due to their interesting electrical properties and a number of promising applications [2 – 4]. Partial substitution of rare earth (Ln^{3+}) by divalent Ba^{2+}, Sr^{2+} and Ca^{2+} ions in the parent $LnMnO_3$ compound induces electronic holes ($p \sim 10^{21}$ cm^{-3}) due to a hopping of electrons between Mn^{3+} and Mn^{4+} ions. At certain doping levels (x $\cong 0.2 \div 0.4$), these materials exhibit paramagnetic to ferromagnetic (PM-FM) phase transition at Curie temperature T_c (100 K $\div$ 390 K), metal-insulator (MI) transition at temperature T_{MI} (just below T_c), as well as colossal magnetoresistance (CMR) and giant piezoresistance effects in the vicinity of T_c. Presence of almost fully spin-polarized carriers in a ferromagnetic state of the manganites is of high interest for various spintronics applications [4]. During the last years, increasing attention was attributed to heterojunctions based on manganite flms grown on conductive substrates such as *n*-type Nb-doped

$SrTiO_3$ [6 – 10]. Significant magnetic field effect on both interface resistance and current-voltage characteristics of the heterojunctions have been reported by a number of authors [3 – 11] although the origin of the interface magnetoresistance is not yet fully understood.

Multiferroics are ferroelectric ferromagnets with coupled electric, magnetic, and structural order parameters coexisting simultaneously in a single phase [12]. This kind of materials demonstrates magnetoelectric effect providing a unique possibility to control electrical and magnetic order parameters via applied electric and magnetic fields [13]. High quality films and heterostructures of the multiferroic materials are expected to be very promising for novel applications as information storage and sensors. Bismuth ferrite, $BiFeO_3$ (BFO) with rhombohedrally distorted perovskite structure is one of the most extensively studied materials of this kind. It is ferroelectric below 1103 K and antiferromagnet below 643 K while thin BFO films demonstrate weak magnetism at room temperature due to G-type canted spin structure [12]. Electrical leakage resulting from possible defects and nonstoichiometry remains as one of the main obstacles to practical applications of the material although it was found recently that electrical conductivity of BFO could be reduced by substitution of both Bi and Fe ions [15 – 17].

Organic semiconductors (OSC) provide new promising possibilities for cheap and mechanically flexible, electronics [18]. The main advantage of the organic materials is relatively simple and low temperature processing of their thin films by using relatively simple techniques such as thermal evaporation and spin coating. Furthermore, organic semiconductors composed of light elements demonstrate unusually large values of spin

---

[*]Corresponding author. Tel.: +370-615-30593; fax.: +370-5-2627123.
E-mail address: *veng@pfi.lt* (B. Vengalis)

relaxation time and therefore they may be used for spintronics applications [19]. Spin-polarized carriers can be injected into OSC from ferromagnetic electrodes or generated via photoexcitation by a circularly polarized light. This provides an interesting possibility for the development of new magnetic field driven optoelectronic devices. One can expect therefore that the combination of ferromagnetic and OSC materials could provide electrical, optical and magnetic functionalities into a single integrated device. Though several hybrid device structures containing OSC and ferromagnetic materials have been reported and various applications of their properties have been pointed out, there is still a lack of knowledge concerning formation and properties of hybrid organic-inorganic heterostructures [20–24]. There is also a need to elucidate possible mechanisms of electrical transport in the interfaces of hybrid heterostructures.

Here in this review, we report major results our recent investigations on both preparation and properties of the heterostructures based on thin films and bilayer structures of magnetic oxides, namely, colossal magnetoresistance lanthanum manganites, $La_{2/3}A_{1/3}MnO_3$ (A = Ca, Sr, Ba, Ce) [9–11], multiferroic $BiFeO_3$ (BFO) [16, 17] and organic (Alq3) compound [22] when grown on conducting Nb-doped $SrTiO_3$ and other substrates (see Table 1). Resistance, magnetoresistance, current-voltage characteristics were measured for the prepared heterojunctions in order to elucidate dominating mechanisms of electrical transport in the interfaces.

Table 1. Major parameters of films and substrate materials used for the investigations: lattice parameters of pseudocubic unit cells, carrier densities and band gap

| Oxide compound	Lattice parameter (nm)	Typical carrier density, cm^{-3}	E_g, eV
$La_{2/3}Sr_{1/3}MnO_3$ (LSMO)	0.387	$p \sim 10^{21}$	
$La_{2/3}Ca_{1/3}MnO_3$ (LCaMO)	0.385	$p \sim 10^{21}$	
$La_{2/3}Ba_{1/3}MnO_3$ (LBMO)	0.391	$p \sim 10^{21}$	
$La_{2/3}Ce_{1/3}MnO_3$ (LCeMO)	0.394	$p \sim 10^{21}$	
$BiFeO_3$ (BFO)	0.396		2.57
$Bi_{0.9}Nd_{0.1}FeO_3$ (BNFO)	0.395		2.62
$LaNiO_3$ (LNO)	0.384	$p \cong 10^{19} \div 10^{21}$	
$SrTiO_3$ (STO)	0.3905	–	
$SrTiO_3\!<\!Nb\!>$ (STON)	$\cong 0.391$	$n \sim 10^{20}$	

2. RESULTS AND DISCUSSION

2.1. Heterostructures based on manganite thin films

Thin films of the lanthanum manganites, $La_{2/3}A_{1/3}MnO_3$ (A = Ca, Sr, Ba, Ce), with thickness ranging from about 100 nm to 200 nm were grown *in-situ* by dc magnetron

sputtering under oxygen pressure $P_{O2} \cong 10\,Pa \div 20\,Pa$ at temperatures $T = (700-750)\,°C$ with following annealing of the grown films in oxygen atmosphere ($P_{O2} \cong 10^5\,Pa$) [9, 10]. Disk-shaped ceramic targets of the same composition have been used for sputtering.

Well defined XRD reflexes of $(n,0,0)$ (n = 1, 2, 3,...) type seen in the measured Θ-2Θ scans revealed epitaxial quality of all manganite films when grown on lattice-matched crystalline $SrTiO_3(100)$ and conducting Nb(0.1 wt.%) – doped $SrTiO_3$. At the same time, polycrystalline quality has been indicated for similar films grown at similar conditions on either Si substrates with preliminary removed native SiO_2 layer or Si coated by conducting $LaNiO_3$ overlayers. Electrical properties of the heterojunctions were investigated by passing current of about 0.01 mA perpendicular to a film plane. In the last case, Ag coatings ($2.0 \times 2.0\,mm^2$) magnetron sputtered onto the tape-like manganite films and metallic In-Ga alloy were used as low contact resistance electrodes for the manganite films and conducting substrates, respectively.

Temperature-dependent resistance of the films, $R(T)$, measured by passing current parallel to a film plane revealed characteristic $R(T)$ peaks at temperatures $T = T_M$ of about 230 K, 330 K, 295 K, 256 K corresponding to the Curie temperature of the prepared Ca, Sr, Ba, Ce- doped manganite films, respectively. At the same time, the prepared $La_{2/3}A_{1/3}MnO_3$ (A = Ca, Sr, Ba, Ce)/STON heterojunctions exhibited temperature-dependent nonlinear current–voltage (I–U) relations and clearly defined rectifying behavior over a wide temperature range both above and below Curie temperature $T_c \cong T_M$ of the manganite films [9].
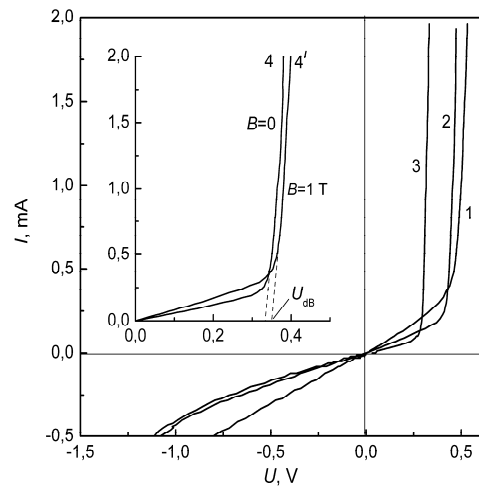

Fig. 1. Current–voltage characteristics of the LBaMO/STON heterojunction measured at $B = 0$ T; T, K: 295 (1), 260 (2), 78 (3) and 230 (4); The $I(U)$ relations at 230 K, $B = 0$ and $B = 1$ T, are shown in the inset

Typical current–voltage I–U characteristics measured for the LBaMO/STON heterojunction at various temperatures in a case of a forward ($U > 0$) and reverse ($U < 0$) bias are displayed in Fig. 1. The highest values of the junction resistance, $R_J(300\,K)$ of about 1 kΩ – 5 kΩ, corresponding to linear I–U relations at low bias voltages (see Fig. 1) have been estimated for the LBMO/STON and

LSMO/STON heterojunctions. Significantly higher values (10 kΩ – 40 kΩ) have been evaluated for similar heterojunctions with Ca-doped manganites while the highest values of the interface resistance (~100 kΩ) demonstrating reduced carrier density at the interface have been estimated for the LaCeMO/STON heterostructures.

Following Fig. 1 we point out an abrupt increase of forward current at a certain voltage U_d representing the build in interfacial potential and known from p-n junction theory as diffusion voltage. Monotonous lowering of the U_d values with temperature decreasing (see curves 1–4 in Fig. 1) has been indicated for all the heterostructures.

A decrease of the junction resistance, R_J, under applied magnetic field corresponding to negative magnetoresistance values (at low forward bias voltages $U << U_d$) were indicated for the heterojunctions in a wide temperature range below the PM-FM transition temperature of the manganite films. Meanwhile, a certain (almost parallel) shift of the $I(U)$ curves to higher voltages with applied magnetic field resulting positive junction magnetoresistance values have been indicated for the heterojunctions at $U > U_d$. Relative increase of the U_d values, i.e. $[U_d(B) - U_d(0)]/U_d(0)$ measured in this work for LCaMO/STON, LCeMO/STON and LBaMO/STON heterojunctions by applying magnetic field $B = 1$ T is shown in Fig. 2, b. Peak-like ($\Delta U_d = U_{d0}$) versus T curves seen from the figure have been explained taking into account strong dependence of the interfacial potential on magnetic field in the temperature region just below the ferromagnetic to paramagnetic phase transition of the manganites.
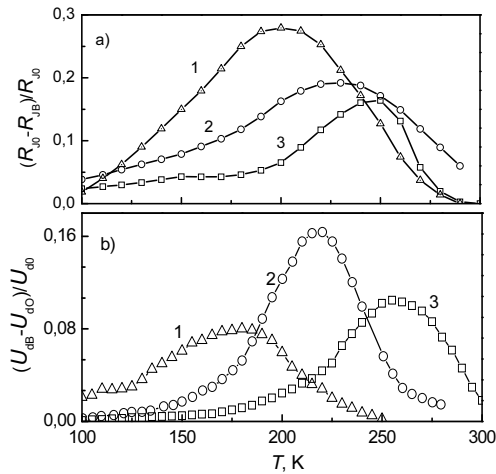
Fig. 2. Junction magnetoresistance (at low bias voltage and $B = 1$ T) (a) and relative increase of the diffusion voltage U_d under applied magnetic field $B = 1.0$ T (b) measured for the LCaMO/STON (1), LCeMO/STON (2) and LBaMO/n-STON (3) heterojunctions

2.2. Thin films and heterostructures of multiferoic BiFeO₃ and Bi₀.₉Nd₀.₁FeO₃

Thin films of BiFeO₃ (BFO) and Bi₀.₉Nd₀.₁FeO₃ (BNFO) with thickness d ranging from about 200 nm to 250 nm were grown *in-situ* at 650-700°C under Ar/O₂ (1:1) gas pressure of 6-10 Pa by RF magnetron sputtering [16].

Wafers of both dielectric SrTiO₃(100), ZrO₂<Y> (YSZ) and conducting crystalline materials, namely, Nb-doped 0.7 weight % SrTiO₃(100) (STON), n-type Si(111) as well as SrTiO₃ coated by highly conductive SrRuO₃ films were used as substrates. Bi content in the ceramic targets was slightly enhanced (by about 5%) to compensate possible loss of highly volatile Bi during film growth.

XRD spectra measured for the undoped BFO/STO(100) films revealed growth of highly oriented perovskite-like BFO phase with certain small part of [110]-axis oriented crystallites and negligible amount of impurity (Bi₃₆Fe₂O₅₇) phase. Meanwhile, similar XRD reflexes of the BNFO films (see Fig. 3) showed single phase material with the off- plane lattice parameter of a pseudocubic unit cell of about 3.95 nm. Thus, our investigations show that partial substitution of Bi^{3+} by Nd^{3+} with slightly reduced ionic radii (r_{Nd}=1.08 Å and r_{Bi}=1.20 Å) stabilizes formation of BiFeO₃ phase and reduces appearance of impurity phases such as Bi₃₆Fe₂O₅₇, Bi₂Fe₄O₉ and Fe₂O₃.

Optical transmittance spectra measured for the BFO/YSZ and BNFO/YSZ films certified presence of a direct bandgap with the characteristic energies E_g of 2.57 eV and 2.62 eV (at T=300 K) for the undoped and Nd-doped materials, respectively [16].
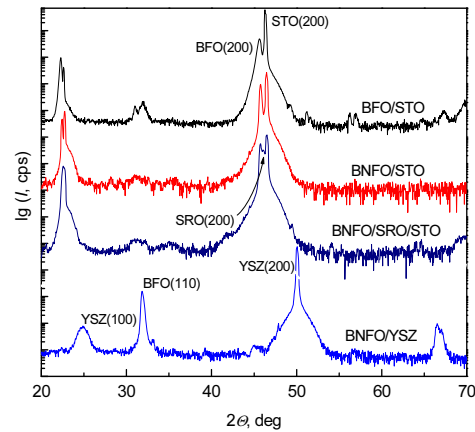

Fig. 3. Θ-2Θ XRD scans of the BiFeO₃ and Bi₀.₉Nd₀.₁FeO₃ films grown by RF magnetron sputtering on crystalline SrTiO₃, YSZ(100) substrates and metallic SrRuO₃/SrTiO₃(100) films

Nonlinear current-voltage (I–U) relations demonstrating rectifying properties have been measured for the Ag/BNFO/STON heterostructures at $T = 300$ K and 78 K (see Fig. 4). At room temperature, linear I–U relation has been measured for the heterostructure at low U values (< 0.2 V) meanwhile a power low: $I \sim U^m$ (with $m \cong 1.5 - 2.2$) has been indicated at $T = 78$ K with U increasing up to about 0.5 V. The increase of differential resistance, $R_d(U = 0)$, from about 1.0 MΩ to 6.0 MΩ have been indicated for the heterostructure with cooling down to 78 K.

The current-voltage dependencies of the heterostructures prepared by growing the BFO and BNFO films on both Nb-doped SrTiO₃(100) demonstrated clearly defined rectifying properties. Linear portion of the ln$I$-U relation indicated for the BNFO/STON heterojunction at $T = 300$ K

(see Fig. 4) demonstrates dominating role of Shottky thermoelectronic emission in the M-I-S diode structure at least at a certain intermediate range of forward bias values while significant deviation from the linear ln I-U relations (at the highest U values) have been explained assuming that current at higher bias voltages is limited by series resistance related either to a bulk resistance of the multiferoic film due to a Poole-Frenkel emission, hopping conduction, space charge-limited conduction and certain additional resistance of electrical contacts.
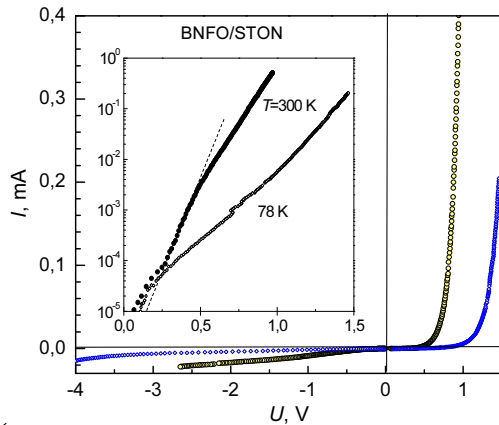
Fig. 4. Current (I) versus voltage (U) relations of the Ag/BNFO/n-SrTiO$_3$<0.7 % Nb> heterostructures measured at 300 K and 78 K. Semilog. plot of the same $I(U)$ dependencies at a forward bias is shown in the inset

The barrier height (Φ_{b0}) of about 0.82 eV and 0.84 eV (derived by fitting numerical I–U curves from the well known Shottky model to the experimental points) have been estimated for the BFO/Si and BNFMO/STON heterostructures at 300 K, respectively. Relatively high values of series resistance estimated for the BFO/Si heterostructure have been explained assuming possible formation of thin SiO$_2$ interlayer in the interface. Complicated shape of the I-U curves of both the BFMMO/STON and (BFO, BNFO)/Si heterostructures measured at $T = 78$ K demonstrates, probably, presence of several electrical transport mechanisms. Following our results, we point out increasing role of space charge limited current in the BFO films with temperature decreasing.

2.3. Heterostructures containing manganite and organic Alq3 semiconductor

Thin films of the organic semiconductor, Alq3, were thermally evaporated in vacuum ($p \approx 4 \times 10^{-6}$ Torr) as top layers onto LSMO-coated SrTiO$_3$ [23]. During film deposition, the substrates were mounted at a distance of about 10 cm from a crucible. Thickness of the as prepared Alq3 films ($d \cong 100$ nm $\div$ 300 nm) was measured by DECTAC profilometer while their surface morphology was studied by atomic force microscopy (AFM).

Deposition through a mask was undertaken to pattern the FM and OS layers in order to prepare the hybrid bilayer structures for electrical measurements. Metallic (Ag) electrodes thermally evaporated both onto the masked OSC

films and LSMO layers were used as electrodes for the electrical measurements. Typical active area of the as prepared hybrid organic on inorganic bilayer heterojunction was about 3 mm^2. Temperature-dependent resistance and magnetoresistance of the LSMO/STO film were measured by passing DC current along the stripe-like LSMO film while 3 point-probe method was applied to measure resistance, magnetoresistance and current-voltage characteristics of the OSC/LSMO interface.

In Fig. 5 we show the current voltage (I–U) dependences, measured for the Alq3/LSMO heterojunctions at $T = 295$ K and 240 K in the absence and presence of a magnetic field ($B = 1.0$ T). In the same temperature range, resistance of the Alq3/LSMO interface (at low bias values) increased gradually with temperature decreasing (in contrast to a decrease of LSMO film resistance in the same temperature range).
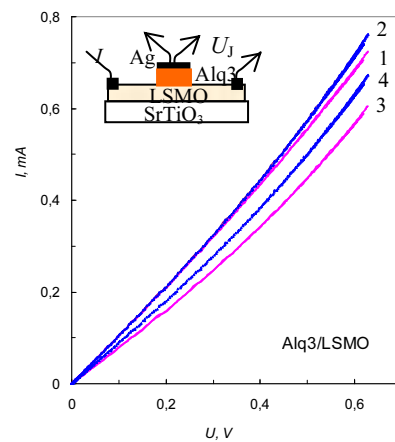
Fig. 5. Current-voltage plots measured for the Alq3/LSMO heterojunctions at $T = 295$ K (1, 2) and 240 K (3, 4) in the absence (1, 3) and presence (2, 4) of magnetic field ($B = 1.0$ T)
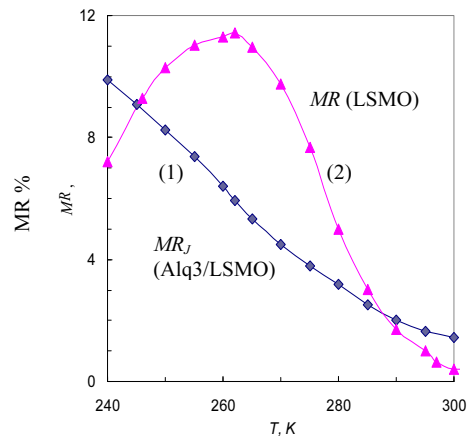
Fig. 6. Junction magnetoresistance (MR$_J$) of the Alq3/LSMO interface (1) and in-plane magnetoresistance (MR) of the LSMO film (2). $B = 1.0$ T

Temperature-dependent magnetoresistance of the Alq3/LSMO interface $MR_J = [R_J(B) - R_J(B{=}0)]/R_J(B = 0)$ measured by applying 3 point-probe method (see inset to Fig. 5) at $B = 1.0$ T with current passing perpendicularly to

a film plane and magnetoresistance of the LSMO film, *MR*, measured by applying current-in-plane geometry are shown in Fig. 6. The highest value of junction magnetoresistance of about 1.5 % has been estimated at room temperature meanwhile higher negative MR_J values (up to about 10 %) have been measured for the Alq3/LSMO interface at 250 K.

To explain nonlinear *I-U* relations (see Fig. 5) and negligible rectifying behavior of the Alq3/LSMO heterojunctions, models of space charge limited current (SCLC) and that of thin potential barrier ($d \sim 1$ nm) in the interface governing tunnelling of carriers between Alq3 and LSMO film have been considered. Tunnel current estimated by applying the well known Simons low was found to be significantly lower compared to the measured current values seen from Fig. 5. Therefore one can conclude that charge transport in the heterostructures is governed mainly by the SCLC process in the organic Alq3 layer. Certainly, a role of space charge may be important in this case as far as carrier density in the FM oxide ($p \sim 10^{21}$ cm^{-3}) is much higher compared to that in the Alq3 compound and density of injected charge carriers is much larger than density of thermally generated free-charge carriers.

3. CONCLUSIONS

We conclude that manganite p-n junctions with clearly defined rectifying behavior have been prepared by growing the LBMO, LCaMO, LSMO and LCeMO films heteroepi-taxially onto Nb 0.1 wt % doped SrTiO$_3$(100). The LaCeMO/STON heterostructures exhibited the highest interface resistance due to reduced carrier density at the interface. All the heterojunctions demonstrated negative magnetoresistance values at low bias values meanwhile positive bias-dependent magnetoresistance have been indicated at $U > U_d$ where U_d is the interfacial potential, corresponding to a steep current increase at a forward bias. The manganite p-n heterojunctions could be promising for the fabrication of planar magnetic field sensor arrays.

High crystalline quality BiFeO$_3$ and Bi$_{0.9}$Nd$_{0.1}$FeO$_3$ films have been grown by RF sputtering on lattice-matched Nb-doped SrTiO$_3$(100). Partial substitution of Bi by Nb revealed increased resistance of the multiferroic films. Nonlinear and clearly defined rectifying properties of the Ag/(BFO, BNFO)/STON heterostructures demonstrated dominating Schottky junction model at $T = 300$ K and increasing role of space charge limited current with T decreasing down to 78 K.

We point out preparation of hybrid organic on inorganic heterojunctions by thermal evaporation of organic Alq3 semiconductor films as top layers onto LSMO manganite films. Significant magnetoresistance values have been indicated for the Alq3/LSMO interface. Charge transport in the Alq3/p-Si heterojunction has been modeled taking into account dominating role of thermoionic emission in a barrier of Schottky type, while mechanisms based on carrier tunnelling through an interfacial barrier and space charge limited current processes were considered to explain nonlinear electrical transport in the Alq3/LSMO heterojunctions.

REFERENCES

1. **Ahn, C. H., Triscone, J.-M., Mannhart, J.** Electric Field Effect in Correlated Oxide Systems *Nature* 424 2003: pp. 1015–1018.

2. **Tokura, Y.** Critical Features of Colossal Magnetoresistive Manganites *Reports on Progress in Physics* 69 2006: pp. 797–851.

3. **Haghiri-Gosnet, A.-M, Renard, J.-P.** CMR Manganites: Physics, Thin Films and Devices *Journal of Physics D: Applied Physics* 36 2003: pp. R127–R150.

4. **Dorr, K.** Ferromagnetic Manganites: Spin-polarized Conduction versus Competing Interactions *Journal of Physics D: Applied Physics* 39 2006: pp. R125–R150.

5. **Nakagawa, N., Asai, M., Mukonoki, Y., Susaki, T., Hwang, H.Y.** Magnetocapacitance and Exponential Magnetoresistance in Manganite-titanate Heterojunctions *Applied Physics Letters* 86 2005: p. 082504.

6. **Sun, J. R., Lai, C. H., Wong, H. K.** Photovoltaic Effect in La$_{0.7}$Ce$_{0.3}$MnO$_{3-delta}$/SrTiO$_3$-Nb Heterojunction and Its Oxygen Content Dependence *Applied Physics Letters* 85 (1) 2004: p. 37.

7. **Wang, D. J., Sun, J. R.. Xie, Y. W, Lü, W. M., Liang, S., Zhao, T. Y, Shen, B. G.** Magnetic Field Effects on the Manganite Junction with Different Electronic Processes *Applied Physics Letters* 91 2007: p. 062503.

8. **Sun, J. R., Shen, G., Tian, H. F., Li, J. Q., Weng, Y. X.** Interfacial Potential and Photoelectronic Properties of Manganite Heterojunction La$_{0.7}$Ce$_{0.3}$MnO$_3$/SrTiO$_3$:Nb *Applied Physics Letters* 87 2005: p. 202502. http://dx.doi.org/10.1063/1.2130724

9. **Vengalis, B., Devenson, J., Šliužienė, K., Butkutė, R., Rosa, M. A., Lisauskas, V., Oginskis, A., Anisimovas, F.** Formation and Investigation of p-n diode Structures Based on Lanthanum Manganites and Nb-doped SrTiO$_3$ *Thin Solid Films* 515 2006: pp. 599. http://dx.doi.org/10.1016/j.tsf.2005.12.253

10. **Devenson, J., Vengalis, B., Lisauskas, V., Oginskis, A. K., Anisimovas, F., Ašmontas, S.** Magnetoresistive Properties of Manganite-Based Heterojunctions *Acta Physica Polonica A* 115 2009: pp. 1130–1132.

11. **Vengalis, B., Rosa, A. M., Devenson, J., Šliužienė, K., Lisauskas, V., Oginskis, A., Anisimovas, F.** Investigation of Heterostructure Formed from Hole- and Electron-doped Lanthanum Manganites *Acta Physica Polonica* A 107 (2) 2005: p. 290–293.

12. **Smolenskii, G. A., Chupis, I. E.** Ferroelectromagnets *Soviet Physics Uspekhi* 25 1982: p. 475. http://dx.doi.org/10.1070/PU1982v025n07ABEH004570

13. **Febig, M.** Revival of Magnetoelectric Effect *Journal of Physics* 38 2005: p. R123.

14. **Wang, J., Neaton, J. B., Zheng, H., Nagarajan, V., Ogale, S. B., Liu, B., Viehland, D., Vaithyanathan, V., Schlom, D. G., Waghmare, U. V., Spaldin, N. A., Rabe, K. M., Wuttig, M., Ramesh, R.** Epitaxial BiFeO$_3$ Multiferroic Thin Film Heterostructures *Science* 299 2003: p. 1719.

15. **Yuan, G. L., Ora, S. W., Liu, J. M., Liu, Z. G.** Size-dependent Structural Preferences and Magnetization Enhancement in 0.5Bi0.8La0.2FeO3–0.5PbTiO3 *Applied Physics Letters* 89 2006: p. 052905.
http://dx.doi.org/10.1063/1.2266992

16. **Vengalis, B., Devenson, J., Oginskis, A. K., Lisauskas, V., Anisimovas, F., Butkutė, R., Dapkus, L.** Optical and Electrical Properties of Nd-doped BiFeO3 Thin Films and Heterostructures *Physica status solidi* 6 2009: pp. 2746 – 2749.

17. **Vengalis, B., Devenson, J., Oginskis, A. K., Lisauskas, V., Dapkus, L., Maneikis, A.** Preparation and Electrical Properties of the $Bi_{0.9}La_{0.1}Fe_{0.9}Mn_{0.1}O_3$/SrTiO$_3$:Nb p-n Heterojunctions *Ferroelectrics* 1563-5112 379 2009: pp. 136 – 143.

18. **Moliton, A.** Opoelectronics of Molecules and Polymers. Springer, New York, 2006: 494 p.
http://dx.doi.org/10.1007/978-0-387-25103-5

19. Organic Spintronics. CRS Press. Taylor and Francis Group, 2010.

20. **Dediu, V., Murgia, M., Matacotta, F. C., Taliani, C., Barbanera, S.** Room Temperature Spin-polarized Injection in Organic Semiconductor *Solid State Communication* 122 2002: p. 181.

21. **Wei, J. H., Guo, Y., Xie, S. J., Mei, L. M., Yan, Y.** Spin-dependent Charge Transport in Organic Semiconductors *Journal of Physics: Conference Ser. 29* 2006: p. 95.

22. **Vengalis, B., Šliužienė, K., Černiukė, I., Butkutė, R., Lisauskas, V., Maneikis, A.** Preparation and Properties of Hybrid Bilayer Structures Based on Organic Alq3, Ferromagnetic $La_{2/3}Sr_{1/3}MnO_3$ and Fe_3O_4 *Proc. SPIE* 7142 2008: p. 71420V.
http://dx.doi.org/10.1117/12.815942

23. **Xiong, Z. H., Wu, D., Vardeny, Z. V., Shi, J.** Giant Magnetoresistance of Organic Spin Valves *Nature* 427 2004: p. 821.

24. **Wang, T. X., Wei, H. X., Zeng, Z. M., Han, X. F., Hong, Z. M., Shi, G. Q.** Magnetic-Nonmagnetic-Magnetic Tunnel Junctions Based on Hybrid Organic LB-films *Applied Physics Letters* 88 2006: p. 242505.
http://dx.doi.org/10.1063/1.2213177